Pure Appl. Chem., Vol. 84, No. 7, pp. 1621–1631, 2012.
http://dx.doi.org/10.1351/PAC-CON-11-10-34

New strategies for natural products containing chroman spiroketals*

Jason C. Green, G. Leslie Burnett IV, and Thomas R. R. Pettus‡

Department of Chemistry and Biochemistry, University of California at Santa Barbara, Santa Barbara, CA 93106-9510, USA

Abstract: Two cycloaddition strategies are described that lead to various chroman spiroketals from assorted exocyclic enol ethers. Unlike conventional thermodynamic ketalization strategies, the stereochemical outcome for this approach is determined by a kinetic cycloaddition reaction. Thus, the stereochemical outcome reflects the olefin geometry of the starting materials along with the orientation of the associated transition state. However, the initial kinetic product can also be equilibrated by acid catalysis and reconstituted into a thermodynamic stereochemical arrangement. Thus, these strategies uniquely enable synthetic access to either the thermodynamic or kinetic conformation of the spiroketal stereocenter itself. Applications of these strategies in the syntheses of berkelic acid, β-rubromycin, and paecilospirone are presented along with the use of a chroman spiroketal for the construction of heliespirones A and C.

Keywords: aromatic; aryl spiroketals; chroman; [4 + 2] cycloaddition; Diels–Alder; natural products; *ortho*-quinone methide; oxidative [3 + 2] cycloaddition; spiroketals; total synthesis.

INTRODUCTION

The chroman spiroketal motif is a unique scaffold found in very few natural products (Fig. 1, **1–6**) [1]. Unlike its aliphatic relatives, the aryl functionality and its three associated sp^2 atoms (2 carbons + 1 oxygen) rigidify the conformation of the associated pyranyl ring. Chroman spiroketals demonstrate a surprising resiliency toward acid-catalyzed equilibration owing to the delocalization of the lone pair of electrons on the chroman oxygen atom through the aromatic ring. Thus, it is difficult for the lone pair of the oxygen atom to assist in the departure of the other protonated oxygen substituent. Additionally, the lone pair of electrons on the chroman oxygen is also difficult to protonate. Thus, cleavage with electron flow proceeding the opposite direction is also thwarted.

The conventional approach for construction of the spiroketal skeleton, **7**, involves dehydration of the appropriately tethered dihydroxyketone precursor **8** (Fig. 2). This involves the creation of both the ethereal spiroketal bonds through sequential additions of the alcohols under reversible conditions to furnish the thermodynamic diastereomer. While this method has been successfully applied to the synthesis of numerous aliphatic spiroketals, it has been shown that many phenols lack the nucleophilicity needed to undergo this transformation [3]. In light of this diminished reactivity, we chose to take an orthogonal approach predicated upon successful cycloaddition reactions employing exocyclic enol ethers. This review discusses the developments pertaining to these two such strategies as presented at

Pure Appl. Chem.* **84, 1543–1667 (2012). A collection of invited papers based on presentations at the 23rd International Conference on Heterocyclic Chemistry (ICHC-23), Glasgow, UK, 31 July–4 August 2011.
‡Corresponding author: E-mail: pettus@chem.ucsb.edu

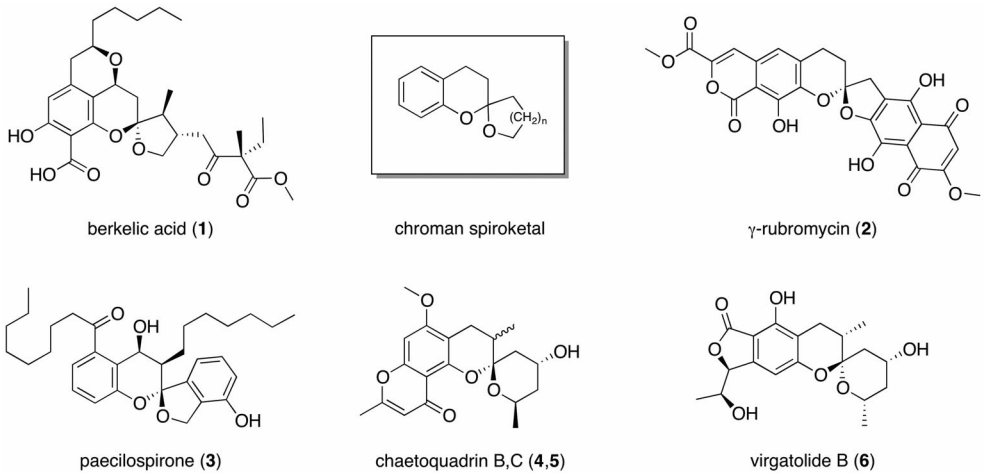

Fig. 1 Representative examples of chroman spiroketal containing natural products.

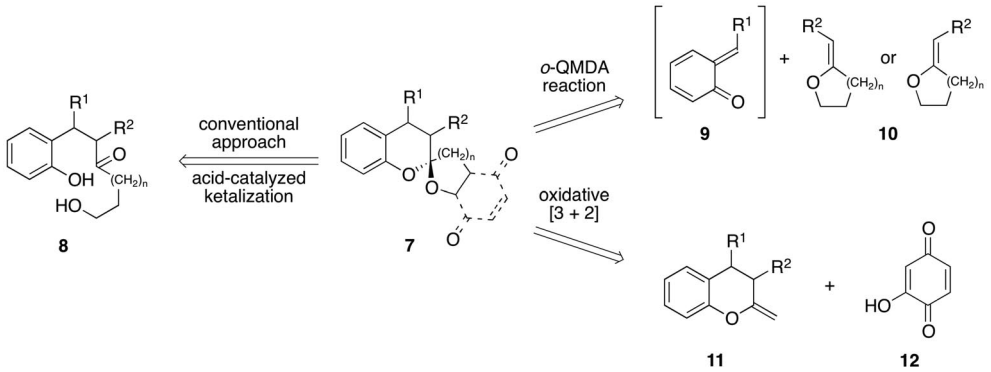

Fig. 2 Comparison of our cycloaddition strategies with the conventional retrosynthesis.

the 23rd International Congress on Heterocyclic Chemistry (ICHC-23). The first strategy builds the chroman ring system by a [4 + 2] reaction between an *ortho*-quinone methide (*o*-QM) intermediate, **9**, and an enol ether, **10** [4]. The second strategy, which is opposite to the first, involves an oxidative [3 + 2] cycloaddition reaction between chroman-derived enol ether **11** and the hydroxybenzoquinone derivative, **12**.

RESULTS AND DISCUSSION

Some time ago, we developed and communicated an elegant cascade reaction that enabled the controlled, low-temperature generation of *o*-QMs [5]. The sequence was initiated by generation of the benzylic alkoxide, **15**, either by nucleophilic addition of a hydride or an organometallic reagent to aldehyde **13** or by deprotonation of benzyl alcohol **14** (Fig. 3). The subsequent carbonate migration and elimination of phenoxide **16** to generate the reactive *o*-QM, **17**, was highly dependent on the metal counterion, allowing us to control the progression of this cascade.

An illustration of this metal dependency was shown by the submission of aldehyde **13** to various hydride reagents (Fig. 4). Addition of $BH_3{\cdot}Me_2S$ simply reduced the aldehyde and furnished alcohol **18** upon work-up [6]. If lithium was present in the solution, as shown with L-selectride, the carbonate

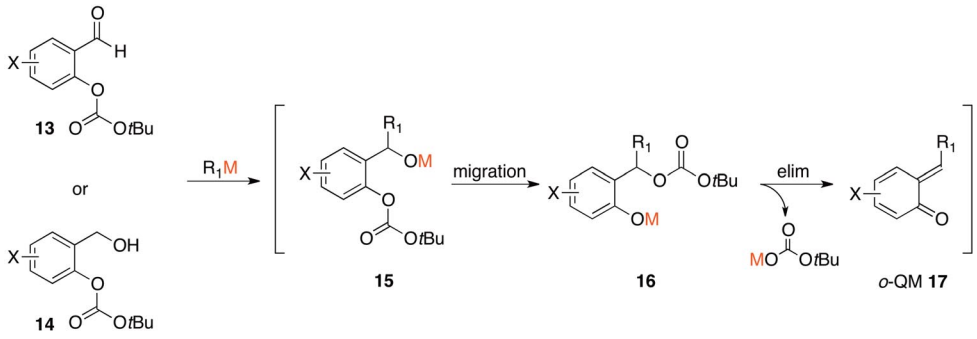

Fig. 3 Generation of the *o*-QM intermediate.

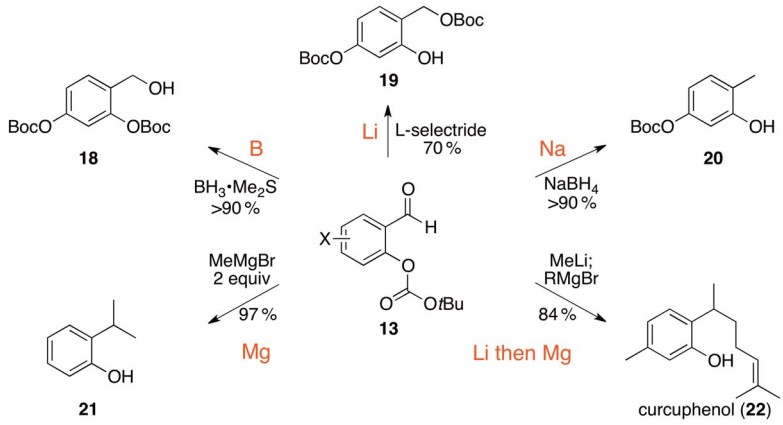

Fig. 4 Taking advantage of the metal dependency of this cascade.

underwent migration upon generation of the benzyl alkoxide to furnish phenol **19**. Reduction of aldehyde **13** with $NaBH_4$ provided phenol **20**. The sodium counterion aided the carbonate migration and its elimination, so as to generate a short-lived *o*-QM that immediately underwent a 1,4-conjugate reduction. Similarly, addition of 2 equiv of a Grignard reagent, such as MeMgBr, initiated the cascade followed by 1,4-conjugate addition, which provided phenol **21**, essentially adding two carbon nucleophiles to the benzylic position. We took advantage of the metal dependency of this sequence by adding two different carbon nucleophiles to the benzylic position. For example, addition of 1 equiv of MeLi to aldehyde **13** resulted in the cascade stopping at intermediate **16** since the lithium phenoxide does not undergo elimination at low temperatures. Next, a Grignard reagent [R = $-(CH_2)_2CHC(CH_3)_2$] was added to the solution. The magnesium catalyzed the elimination, and the resulting *o*-QM underwent 1,4-conjugate addition by the second organometallic reagent, providing curcuphenol (**22**) [7].

Later we used this procedure to demonstrate the first examples of diastereoselective *o*-QM cycloadditions. We found that these inverse demand Diels–Alder (DA) reactions significantly favor the *endo*-transition state with electron-rich alkenes [8]. As shown in Fig. 5, addition of PhMgBr to aldehyde **23** initiated the cascade sequence in which the resulting *o*-QM intermediate underwent a cycloaddition with ethyl vinyl ether **24**, which furnished chroman **25** in >20:1 dr. The process proved quite general and far more convenient than previous methods involving *o*-QMs. Since the cycloaddition occurred between –78 and –10 °C, it was much more sensitive to electronic and steric effects and proceeded with better selectivity than previous methods. The cycloaddition reaction was amenable toward reactions with various electron-rich double bonds such as styrenes, enamines, and imines including

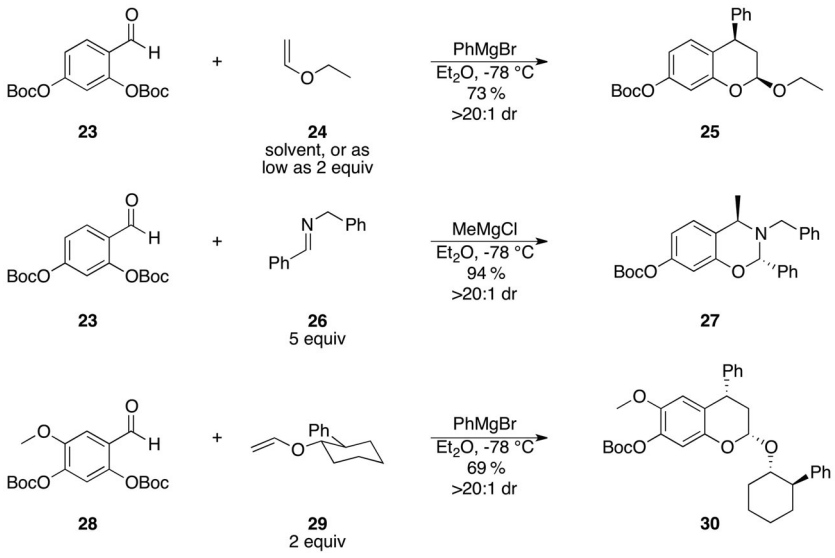

Fig. 5 *o*-QMDA reactions.

compound **26**. The latter furnished oxazine **27**. Next, we provided the first example of an asymmetric cycloaddition of an *o*-QM intermediate [9]. Addition of PhMgBr to aldehyde **28** in the presence of enol ether **29** afforded the cycloadduct, **30**. This enantioselective strategy was successfully applied to multiple total syntheses including the natural products (+)-mimosifoliol, (+)-tolterodine, and (–)-curcuphenol.

On the basis of these findings, we speculated that exocyclic enol ethers would participate in this *o*-QMDA reaction to furnish chroman spiroketals [10]. Unlike conventional ketalizations that furnish only the thermodynamic diastereomer, the stereochemical outcome of our reaction would be governed by the geometry of the enol ether starting material in relation to the intervening transition state. This approach would allow us to target either thermodynamic or kinetic spiroketals. As expected, deprotonation of alcohol **31** with *t*-BuMgCl initiated the cascade, and the subsequent cycloaddition reaction with enol ether **32** furnished the chroman spiroketal, **33** (Fig. 6). We also demonstrated a diastereoselective variant of this cycloaddition with enol ether **34**, which provided spiroketal **35**.

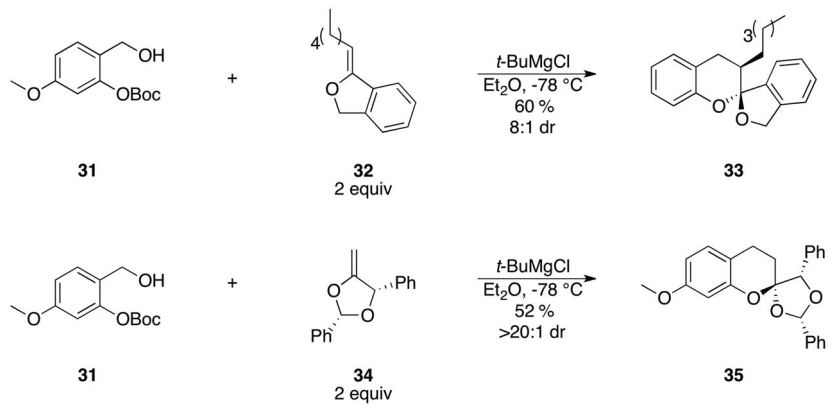

Fig. 6 *o*-QMDA reaction to chroman spiroketals.

Berkelic acid

Among the first targets for application of this new strategy was berkelic acid (**1**), a natural product whose initial assignment as the kinetic 5,6-chroman spiroketal piqued our interest, though it was later revised to the thermodynamic diastereomer during the course of our studies (Fig. 7) [1a,11]. The natural product's complexity required some modifications to our original method. With the benzylic ethereal stereocenter in mind, we designed *o*-QM precursor **36**, which contained a tethered acetate leaving group [12]. Deprotonation of the phenol with *t*-BuMgCl resulted in an elimination to generate an *o*-QM that underwent a [4 + 2] cycloaddition with exocyclic enol ether **37** to afford the respective spiroketals in a 3:1 ratio favoring the *endo* kinetic isomer. Treatment of this mixture with trifluoroacetic acid (TFA) resulted in an equilibration of the spiroketal stereocenter to afford a 1:10 diastereomeric ratio favoring the thermodynamic spiroketal, **38**. The tethered carboxylic acid then served to trap the cation that resulted from a benzylic oxidation to afford the final ring of the tetracyclic lactone, **39**.

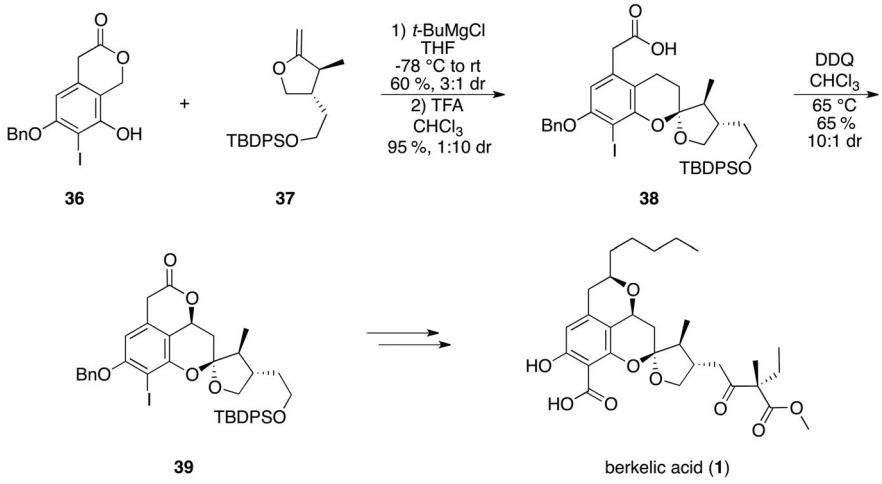

Fig. 7 Synthesis of berkelic acid.

ent-Heliespirone A and C

Correlation of this method to the syntheses of *ent*-heliespirones A (**45**) and C (**46**) was not as straightforward [13]. Our plan was to perform a diastereoselective reduction of a chroman spiroketal as a means to create the *cis*-2,4-disubstitution displayed in the chroman intermediate **44** (Fig. 8) [14].

Deprotonation of phenol **40** with MeMgBr initiated the *o*-QMDA reaction with exocyclic enol ether **41** and afforded the chroman spiroketal, **42**, in >20:1 dr. As expected in the following reduction, A-1,3 interactions served to position the benzylic substituent in a *pseudo*-axial orientation, so that hydride addition to the oxonium intermediate proceeded from the opposite face to afford the *cis*-2,4-disubstituted chroman, **43**, as a single diastereomer. Identical stereoguidance from the benzylic stereocenter was observed if the methyl stereocenter in the dioxolane ring was absent during the reduction reaction. This two-step process successfully installed the two key stereocenters that were used to complete the total syntheses.

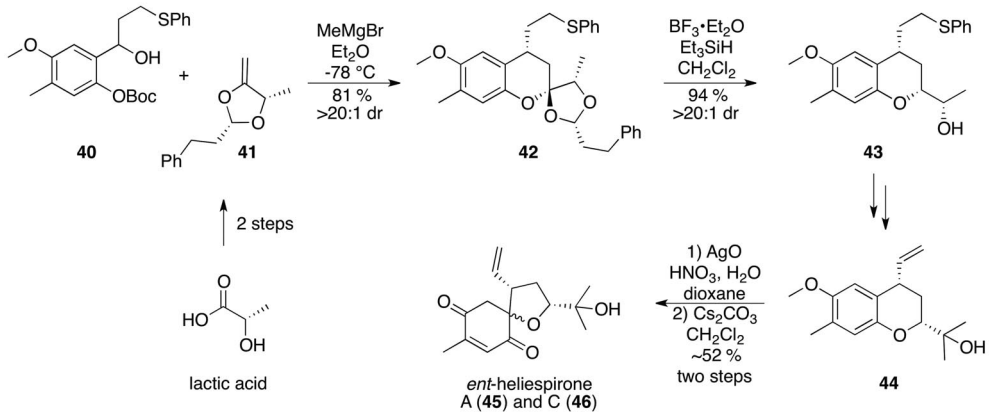

Fig. 8 Heliespirones.

Paecilospirone

Our retrosynthetic plan for paecilospirone (**3**) involves a late-stage benzylic oxidation of the tetracyclic intermediate, **47** (Fig. 9) [15]. The key step once again featured the creation of the central chroman spiroketal through a cycloaddition reaction between an intermediate *o*-QM, **48**, and an exocyclic enol ether, **49**.

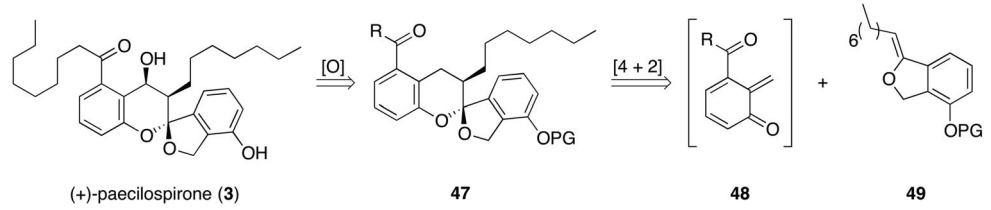

Fig. 9 Paecilospirone retrosynthesis.

An initial model study successfully fused alcohol **31** with enol ether **32** (Fig. 10). The reaction provided compound **33** with the desired chroman spiroketal [10b]. For the actual synthesis, we needed to incorporate the octyl residue onto the *o*-QM coupling partner. We had imagined a route to generate the *o*-QM by addition of the alkyl residue as an organometallic reagent to the cyclic ester, **50**, ($n = 0$) to free a benzylic alkoxide and trigger the cycloaddition with enol ether **51**. As fate would have it, the reaction proceeded when $n = 1$ and failed to give any of the desired product, **52**, when $n = 0$. Our next approach involved a version of the tethered acetate approach we had successfully applied to the synthesis of berkelic acid (**1**). Unfortunately, constricting the cyclic ester from a six- to a five-membered ring may have misaligned the orbitals such that the key elimination could not occur. Thus, we did not see any of the desired chroman adduct, **55**, upon deprotonation of **53** with *t*-BuMgCl in the presence of enol ether **54**.

Our current approach involves deprotonation of alcohol **56** in the presence of enol ether **54** (Fig. 11). With the tetracyclic skeleton, **57**, intact, we are currently focused on installation of the octyl side chain and the final benzylic oxidation.

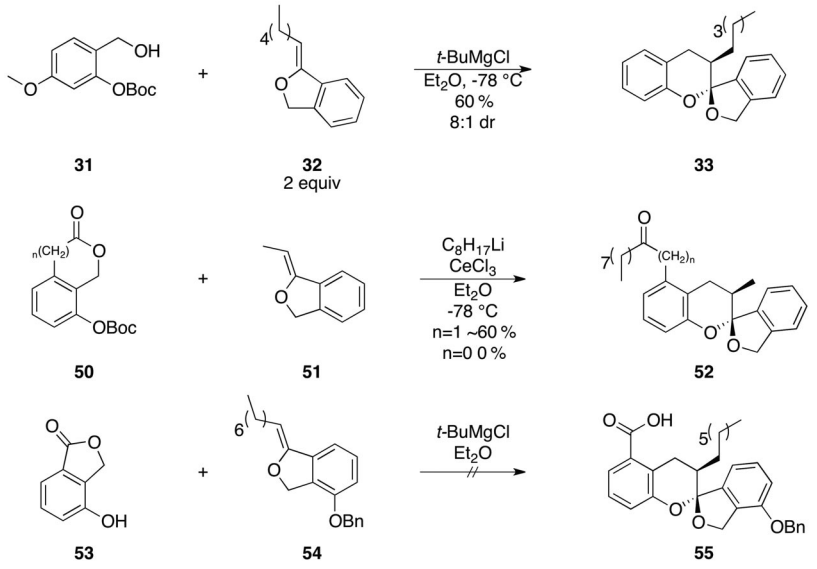

Fig. 10 Attempted *o*-QMDA reactions.

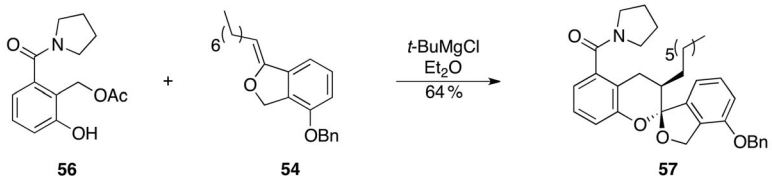

Fig. 11 Successful *o*-QMDA reaction.

γ-Rubromycin

γ-Rubromycin (**2**) initially appeared to be the perfect target for application of our cycloaddition strategy [16]. Our first approach involved a union of the left, **58**, and right, **59**, hemispheres through an *o*-QMDA reaction to build the central chroman spiroketal in a highly convergent manner (Fig. 12).

The first model study involved deprotonation of alcohol **31** with *t*-BuMgCl in the presence of enol ether **62** (Fig. 13). The desired cycloadduct, **63**, was obtained in a meager 10 % yield along with the benzofuran, **64**. Presumably, the fragile enol ether, **62**, succumbs to isomerization under these conditions. To circumvent this unfortunate reactivity, we employed a more stable enol ether, **65**, that might subsequently undergo an acid-catalyzed rearrangement to furnish the desired 6,5-spiroketal. The cycloaddition reaction and reductive deprotection proceeded as expected to furnish spiroketal **66**. Subsequent treatment of **66** with a cadre of Lewis acids, failed to afford the desired spiro-adduct, **67**. In most instances, the starting material remained unchanged or suffered decomposition.

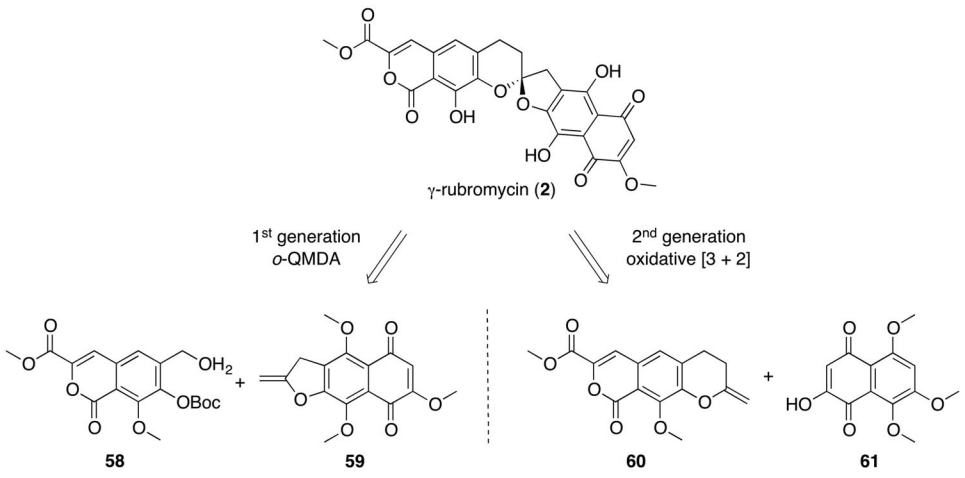

Fig. 12 First- and second-generation retrosyntheses.

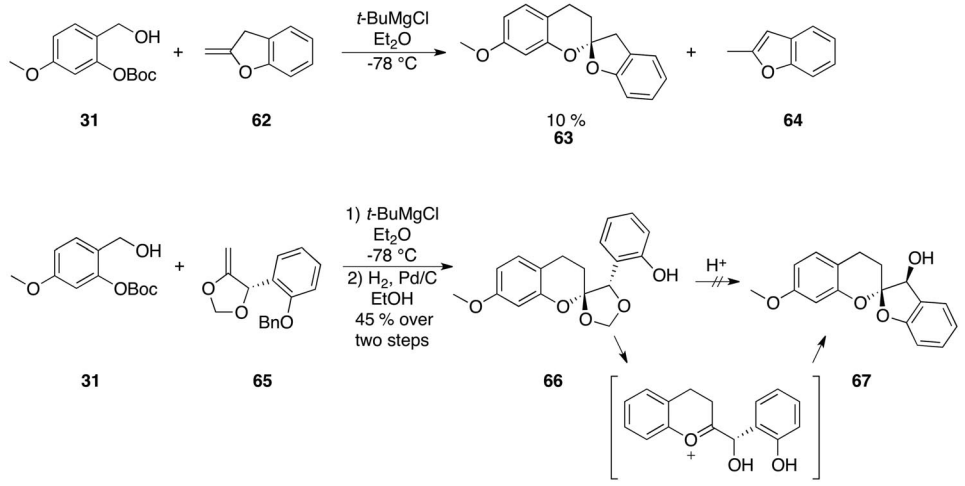

Fig. 13 γ-Rubromycin model studies.

Although discouraged by these results, we remained confident that the most efficient route to build this natural product would involve a coupling reaction through the central chroman spiroketal. After an exhaustive search of the literature, we came across an example of an oxidative [3 + 2] cycloaddition between enol ether **68** and cyclohexane-1,3-dione, **69**, that furnished the tricycle, **70** (Fig. 14) [17]. This approach provided a strategy where the chroman ring contained the enol ether, and the cycloaddition reaction would construct the furan. To our delight, submission of exocyclic enol ether **71** and cyclohexane-1,3-dione, **69**, to similar oxidative conditions afforded spiroketal **72** [18]. We also demonstrated that this reaction was susceptible to diastereocontrol by incorporating a directing group into the enol ether, **73**. This guided the hydroxynapthoquinone, **74**, to approach from one face of the enol ether during the cycloaddition reaction and furnished chroman spiroketal **75** as single diastereomer [19].

These results prompted our second-generation retrosynthesis to take advantage of this oxidative format in which the two coupling partners, exocyclic enol ether **60** and hydroxynapthoquinone **61**, were polar opposites of the first strategy (Fig. 15) [20]. This oxidative cycloaddition reaction provided the

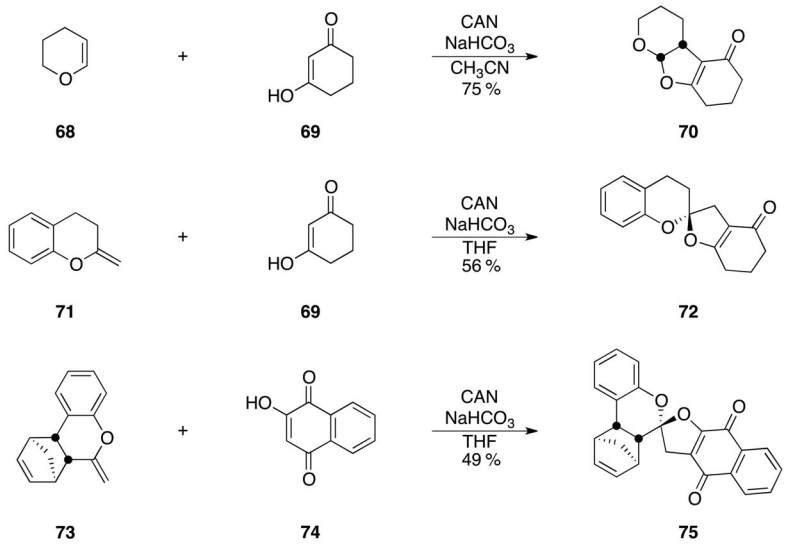

Fig. 14 Oxidative [3 + 2] cycloaddition reaction.

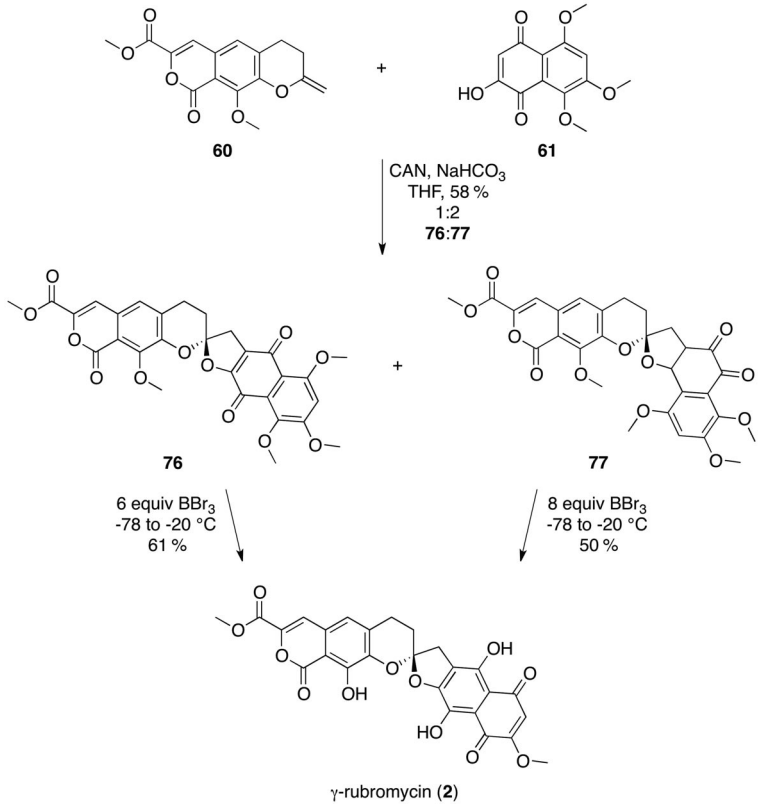

Fig. 15 Successful strategy to γ-rubromycin.

expected *para*-quinone, **76**, as well as compound **77**, presumably by a cycloaddition of the *ortho*-quinone tautomer of **61**. Fortunately, BBr_3 catalyzed the *O*-alkyl deprotections and an *ortho*- to *para*-quinone rearrangement of **77**, allowing us to funnel both cycloaddition products to γ-rubromycin (**2**).

CONCLUSION

We have successfully developed two cycloaddition strategies to construct chroman spiroketals from exocyclic enol ethers. The most significant advantage to this approach was the ability to control the final stereochemical conformation of the anomeric center by choosing the olefin geometry of the starting materials. This allowed us synthetic access to not only the natural thermodynamic diastereomer, which was the sole product from an acid-catalyzed ketalization reaction, but also the kinetic diastereomer if so desired. We demonstrated the flexibility of our *o*-QMDA chemistry and developed a polar opposite approach involving an oxidative [3 + 2] cycloaddition to address the instability of specific enol ethers.

REFERENCES

1. (a) A. A. Stierle, D. B. Stierle, K. Kelly. *J. Org. Chem.* **71**, 5357 (2006); (b) H. Brockmann, W. Lenk, G. Schwantje, A. Zeeck. *Tetrahedron Lett.* **7**, 3525 (1966); (c) H. Brockmann, W. Lenk, G. Schwantje, A. Zeeck. *Chem. Ber.* **102**, 126 (1969); (d) H. Brockmann, A. Zeeck. *Chem. Ber.* **103**, 1709 (1970); (e) C. Puder, S. Loya, A. Hizi, A. Zeeck. *Eur. J. Org. Chem.* 729 (2000); (f) M. Namikoshi, H. Kobayashi, T. Yoshimoto, S. Meguro. *Chem. Lett.* **29**, 308 (2000); (g) M. Namikoshi, H. Kobayashi, T. Yoshimoto, S. Meguro, K. Akano. *Chem. Pharm. Bull.* **48**, 1452 (2000); (h) H. Fujimoto, M. Nozawa, E. Okuyama, M. Ishibashi. *Chem. Pharm. Bull.* **50**, 330 (2002); (i) J. Li, L. Li, Y. Si, X. Jiang, L. Guo, Y. Che. *Org. Lett.* **13**, 2670 (2011).
2. J. Sperry, Z. E. Wilson, D. C. K. Rathwell, M. A. Brimble. *Nat. Prod. Rep.* **27**, 1117 (2010).
3. (a) M. Brasholz, S. Sörgel, C. Azap, H.-U. Reißig. *Eur. J. Org. Chem.* 3801 (2007); (b) S. P. Waters, M. W. Fennie, M. C. Kozlowski. *Org. Lett.* **8**, 3243 (2006); (c) C. Venkatesh, H.-U. Reißig. *Synthesis* 3605 (2008).
4. For a comprehensive review of *ortho*-quinone methides: R. W. Van De Water, T. R. R. Pettus. *Tetrahedron* **58**, 5367 (2002).
5. R. W. Van De Water, D. J. Magdziak, J. N. Chau, T. R. R. Pettus. *J. Am. Chem. Soc.* **122**, 6502 (2000).
6. R. M. Jones, R. W. Van De Water, C. C. Lindsey, C. Hoarau, T. Ung, T. R. R. Pettus. *J. Org. Chem.* **66**, 3435 (2001).
7. (a) J. C. Green, T. R. R. Pettus. *J. Am. Chem. Soc.* **133**, 1603 (2011); (b) K. Tuttle, A. A. Rodriguez, T. R. R. Pettus. *Synlett* 2234 (2003); (c) C. C. Lindsey, T. R. R. Pettus. *Tetrahedron Lett.* **47**, 201 (2006).
8. (a) R. M. Jones, C. Selenski, T. R. R. Pettus. *J. Org. Chem.* **67**, 6911 (2002); (b) C. C. Lindsey, T. R. R. Pettus. *Tetrahedron Lett.* **47**, 201 (2006).
9. (a) C. Selenski, L. H. Mejorado, T. R. R. Pettus. *Synlett* 1101 (2004); (b) C. Selenski, T. R. R. Pettus. *J. Org. Chem.* **69**, 9196 (2004); (c) J. C. Green, S. Jiménez-Alonso, E. R. Brown, T. R. R. Pettus. *Org. Lett.* **13**, 5500 (2011).
10. (a) Y. Huang, T. R. R. Pettus. *Synlett* 1353 (2008); (b) M. A. Marsini, Y. Huang, C. C. Lindsey, K.-L. Wu, T. R. R. Pettus. *Org. Lett.* **10**, 1477 (2008).
11. (a) P. Buchgraber, T. N. Snaddon, C. Wirtz, R. Mynott, R. Goddard, A. Fürstner. *Angew. Chem., Int. Ed.* **47**, 8450 (2008); (b) T. N. Snaddon, P. Buchgraber, S. Schulthoff, C. Wirtz, R. Mynott, A. Fürstner. *Chem.—Eur. J.* **16**, 12133 (2010).
12. T. A. Wenderski, M. A. Marsini, T. R. R. Pettus. *Org. Lett.* **13**, 118 (2011).

13. (a) F. A. Macías, R. M. Varela, A. Torres, J. M. G. Molinillo. *Tetrahedron Lett.* **39**, 427 (1998); (b) F. A. Macías, J. L. G. Galindo, R. M. Varela, A. Torres, J. M. G. Molinillo, F. R. Fronczek. *Org. Lett.* **8**, 4513 (2006).
14. W.-J. Bai, J. C. Green, T. R. R. Pettus. *J. Org. Chem.* **77**, 379 (2012).
15. Unpublished work by Mr. Leslie Burnett.
16. (a) H. Brockmann, W. Lenk, G. Schwantje, A. Zeeck. *Tetrahedron Lett.* **7**, 3525 (1966); (b) H. Brockmann, W. Lenk, G. Schwantje, A. Zeeck. *Chem. Ber.* **102**, 126 (1969); (c) H. Brockmann, A. Zeeck. *Chem. Ber.* **103**, 1709 (1970); (d) C. Puder, S. Loya, A. Hizi, A. Zeeck. *Eur. J. Org. Chem.* 729 (2000).
17. S. C. Roy, P. K. Mandal. *Tetrahedron* **52**, 12495 (1996).
18. C. C. Lindsey, K.-L. Wu, T. R. R. Pettus. *Org. Lett.* **8**, 2365 (2006).
19. K.-L. Wu, S. Wilkinson, N. O. Reich, T. R. R. Pettus. *Org. Lett.* **9**, 5537 (2007).
20. K.-L. Wu, E. V. Mercado, T. R. R. Pettus. *J. Am. Chem. Soc.* **133**, 6114 (2011).

